S1 Supplementary Figures

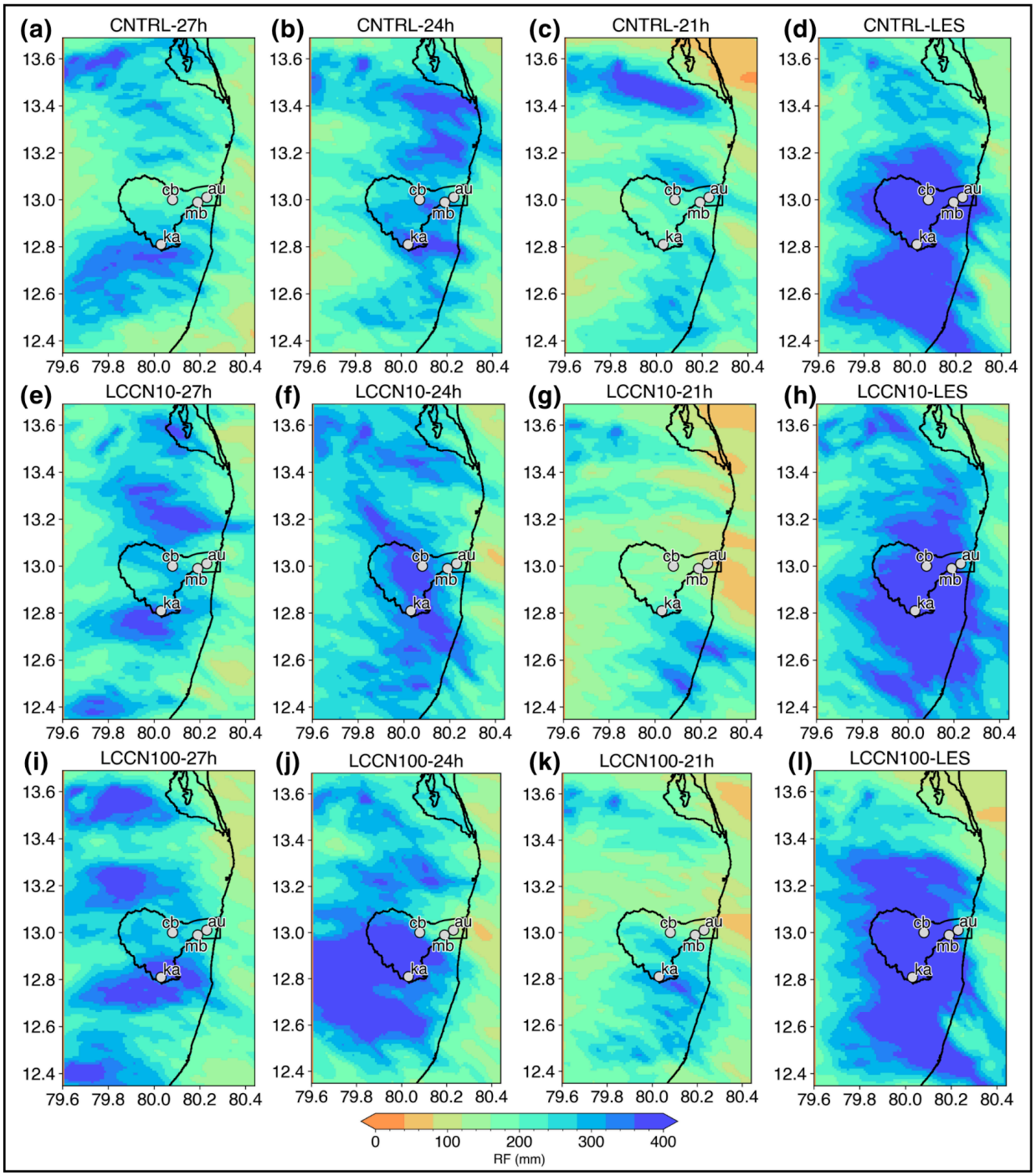

Fig. S1. Spatial distribution of accumulated rainfall for all sensitivity experiments: CNTRL(a-d), LCCN10 (e-h), and LCCN100 (i-l) experiments

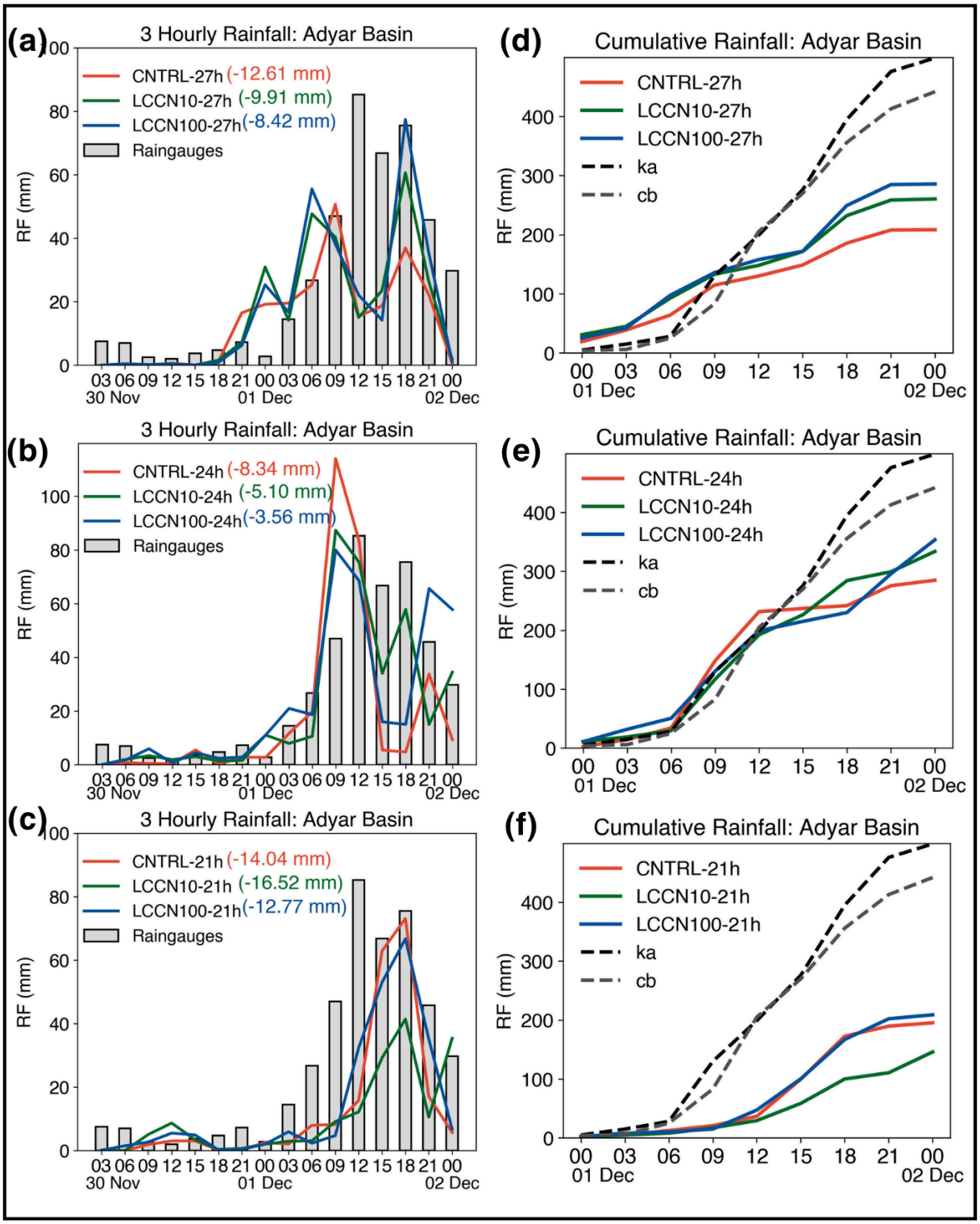

Fig. S2. Left panels show 3-hourly accumulated rainfall with mean biases (mm) over the Adyar basin for sensitivity experiments at lead times of (a) 27 hours, (b) 24 hours, and (c) 21 hours, evaluated against raingauge observations at the basin. Right panels show the corresponding basin-averaged cumulative rainfall for (d) 27 hours, (e) 24 hours, and (f) 21 hours

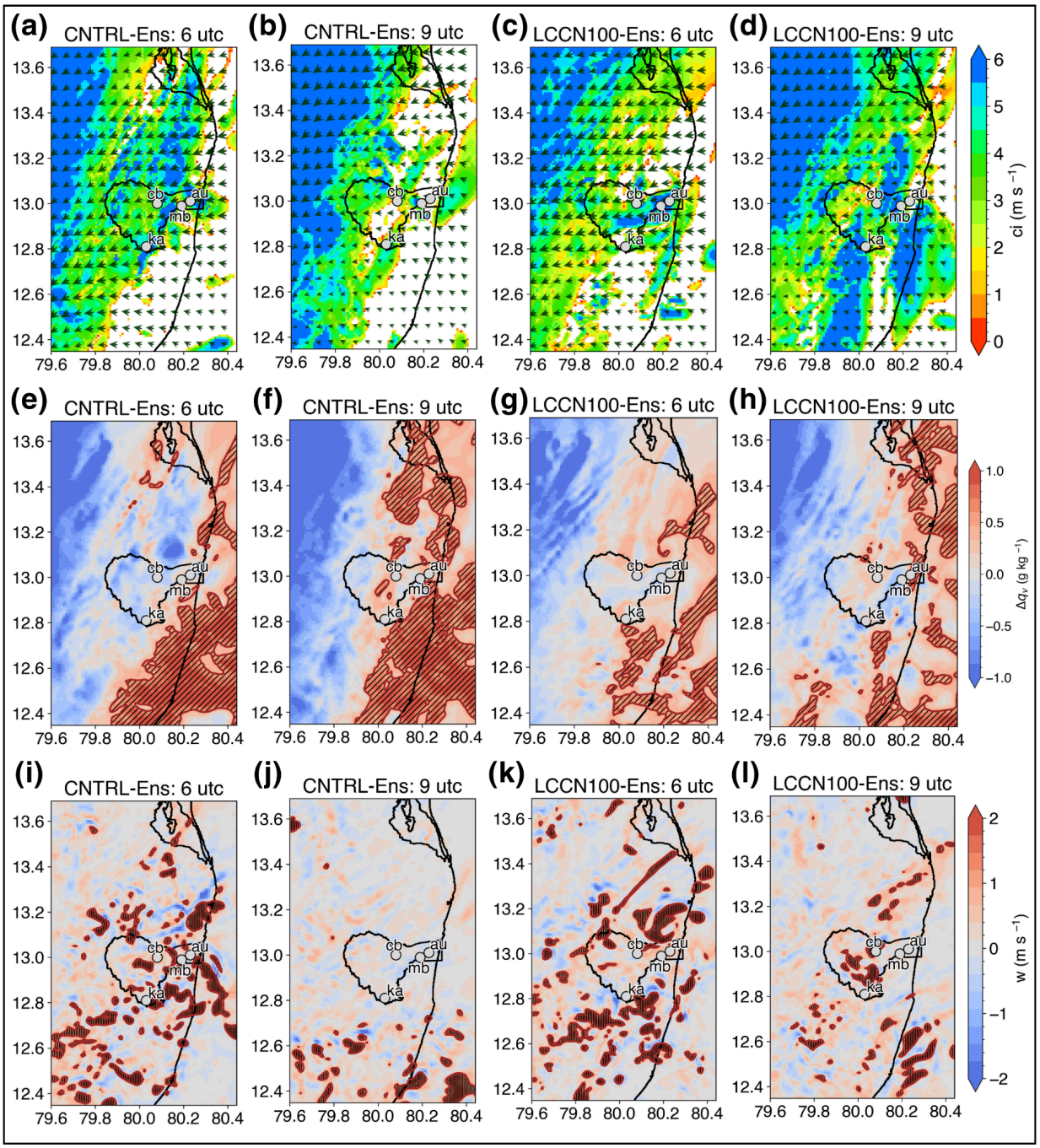

Fig. S3. The spatial distribution of cold pool intensity (a-d), moisture patch (e-h) and convective updraft (red) cores (i-r) at 650 hpa at 6 UTC and 9 UTC on 1 December for CNTRL-Ens and LCCN100-Ens

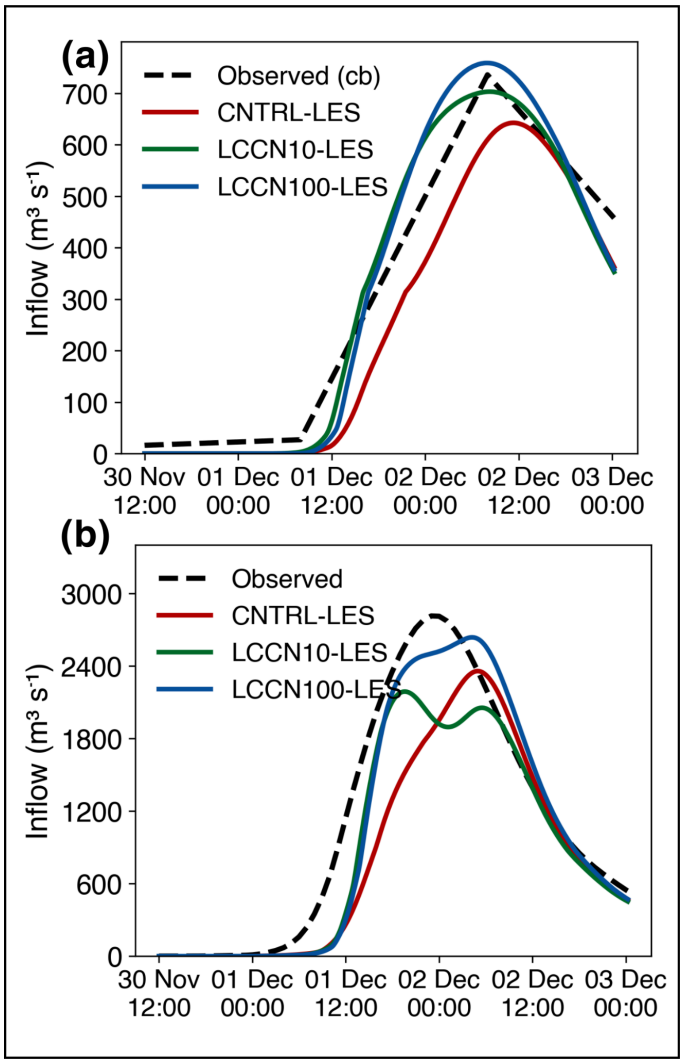

Fig. S4. The comparison of IMERG derived observed peak inflows with simulated peak inflows from CNTRL-LES, LCCN10-LES, and LCCN100-LES into (a) cb reservoir and (b) Chennai city

S2 Supplementary Tables

Inner Domain	**Aerosol (CCN) Experiments**	**Model Initialization, (domains)**	**Sensitivity Experiments**	**Ensemble (1 km)**
1km (d4)	CNTRL(baseline), LCCN10-CNTRL/10, LCCN100-CNTRL/100	28 Nov, 21 UTC (d1-d4) Lead time: 27 hrs	CNTRL-27h, LCCN10-27h, LCCN100-27h	CNTRL-Ens, LCCN10-Ens, LCCN100-Ens
		29 Nov, 00 UTC (d1-d4) Lead time: 24 hrs	CNTRL-24h, LCCN10-24h, LCCN100-24h	
		29 Nov, 03 UTC (d1-d4) Lead time: 21 hrs	CNTRL-21h, LCCN10-21h, LCCN100-21h	
0.2 km (d5)		29 Nov, 00 UTC (d1-d4) 1 Dec, 00 UTC (d5)	CNTRL-LES, LCCN10-LES, LCCN100-LES	-

Table S1 summarizes the sensitivity experiments based on aerosol (CCN) emissions and model initialization in WRF

	CNTRL -27h	**LCCN10 -27h**	**LCCN100 -27h**	**CNTRL -24h**	**LCCN10 -24h**	**LCCN100 -24h**
Bias	-98.65	-82.14	-74.44	-81.12	-63.36	-59.34
% change DEF-27h	-	16.74	24.54	NA	NA	NA
% change DEF-24h	NA	NA	NA	-	21.90	26.80
% change 27h-24h	-	-	-	17.35	23.17	20.27

Table S2 presents the spatial bias (mm) in accumulated rainfall over domain d4 for lead times of 27 hours (CNTRL-27h, LCCN10-27h, and LCCN100-27h) and 24 hours (CNTRL-24h, LCCN10-24h, and LCCN100-24h), evaluated against IMERG observations after spatial regridding. The table also reports the percentage improvement of each sensitivity experiment relative to the respective baseline (CNTRL) configuration at both 27-hour and 24-hour lead times. In addition, the final row quantifies the improvement of each experiment when lead time is reduced from 27 hours to 24 hours

Period	Date	Location	Precipitation	Surface CCN (Daily Mean Conc)
Low Rainfall	26th Nov	80.0°E, 13.0°N	1.550 mm	3.67 x 10^9 (#/kg)
		80.0°E, 13.5°N	0.638 mm	5.82 x 10^9 (#/kg)
	27th Nov	80.0°E, 13.0°N	1.471 mm	5.29 x 10^9 (#/kg)
		80.0°E, 13.5°N	0.586 mm	5.69 x 10^9 (#/kg)
	28th Nov	80.0°E, 13.0°N	6.14 mm	5.22 x 10^9 (#/kg)
		80.0°E, 13.5°N	4.64 mm	5.61 x 10^9 (#/kg)
Moderate to Extreme Rainfall	29th Nov	80.0°E, 13.0°N	36.609 mm	2.20 x 10^9 (#/kg)
		80.0°E, 13.5°N	42.782 mm	2.89 x 10^9 (#/kg)
	30th Nov	80.0°E, 13.0°N	55.985 mm	2.94 x 10^9 (#/kg)
		80.0°E, 13.5°N	45.782 mm	3.87 x 10^9 (#/kg)
	1st Dec	80.0°E, 13.0°N	139.874 mm	9.09 x 10^8 (#/kg)
		80.0°E, 13.5°N	116.170 mm	1.03 x 10^9 (#/kg)
	2nd Dec	80.0°E, 13.0°N	37.203 mm	2.14 x 10^9 (#/kg)
		80.0°E, 13.5°N	32.684 mm	2.51 x 10^9 (#/kg)
	3rd Dec	80.0°E, 13.0°N	21.906 mm	4.07 x 10^9 (#/kg)
		80.0°E, 13.5°N	13.883 mm	5.19 x 10^9 (#/kg)

Table S3 shows daily precipitation data and daily mean surface CCN concentrations from MERRA2, comparing the two periods of rainfall at two locations in and around Chennai during the pre-analysis study

Aerosol type	Effective radius r[µm]	Density (gm^{-3})
Hydrophilic BC	0.036	1000
Hydrophilic OC	0.087	1800
Sea Salt (Bin 2)	0.3	2200
Sea Salt (Bin 3)	1.0	2200
Sea Salt (Bin 3)	3.25	2200
Sea Salt (Bin 4)	7.5	2200
Sulfate (SO4)	0.242	1700

Table S4 shows water-friendly aerosol components in GOCART with effective radius and density at 550 nm (Lu et al., 2022)

S3 Supplementary Methods

S3.1 Moisture Patch Identification and analysis of Cold Pool dynamics

The cold pool extent is calculated from Eq. (S1) from 56 m (z_1) to 540 m (z_2), where the change in equivalent potential temperature ($\Delta\theta e$) is less than 2K (Schlemmer and Hohenegger, 2014).

$$\Delta\theta_e(x,y) = \frac{1}{z2-z1}\left[\int_{z1}^{z2}\theta_e(x,y,z)\,dz - \overline{\int_{z1}^{z2}\theta_e(x,y,z)\,dz}\right] \quad \text{(S1)}$$

where $x, y,$ and z denote the horizontal, meridional, and vertical direction.

The intensity of the cold pool (ci) is calculated from the cold pool extent shown in Eq. (S2).

$$ci = \sqrt{(z2 - z1)}\; g\frac{-\Delta\theta_e}{\theta_{e,surface}} \quad \text{(S2)}$$

where g is the acceleration due to gravity and $\theta_{e,surface}$ is equivalent potential temperature at the surface. The spatial extent of the moisture patch is calculated similarly from Eq. (S1), where a change in water vapor content (Δq_v) exceeds 0.5 g kg^{-1} (Schlemmer and Hohenegger, 2014).

S3.2 Surface emissions estimation from MERRA2

Surface-level aerosol concentrations are estimated using MERRA2 mixing ratios (kg kg^{-1}) and size distribution parameters. The GOCART model includes the following water-friendly aerosol types: hydrophilic black carbon (BC), hydrophilic organic carbon (OC), four bins of sea salt, and sulfates (Table S4).

Concentrations of BC (#kg^{-1}) = (BC Aerosol Mixing Ratio) ÷ (4/3 × π × (0.036 × 10^{-6})^3) × 1000)
Concentrations of OC (#kg^{-1}) = (OC Aerosol Mixing Ratio) ÷ (4/3 × π × (0.087 × 10^{-6})^3) × 1800)
Concentrations of SS1 (#kg^{-1}) = (SS1 Aerosol Mixing Ratio) ÷ (4/3 × π × (0.3 × 10^{-6})^3) × 2200)
Concentrations of SS2 (#kg^{-1}) = (SS2 Aerosol Mixing Ratio) ÷ (4/3 × π × (1.0 × 10^{-6})^3) × 2200)
Concentrations of SS3 (#kg^{-1}) = (SS3 Aerosol Mixing Ratio) ÷ (4/3 × π × (3.25 × 10^{-6})^3) × 2200)
Concentrations of SS4 (#kg^{-1}) = (SS4 Aerosol Mixing Ratio) ÷ (4/3 × π × (7.5 × 10^{-6})^3) × 2200)
Concentrations of SO4 (#kg^{-1}) = (SO4 Aerosol Mixing Ratio) ÷ (4/3 × π × (0.242 × 10^{-6})^3) × 1700) (S3)

Total Concentrations (#kg^{-1}) = BC (#kg^{-1}) + OC (#kg^{-1}) + SS1 (#kg^{-1}) + SS2 (#kg^{-1}) + SS3 (#kg^{-1}) + SS4 (#kg^{-1}) + SO4 (#kg^{-1}) (S4)

The surface emissions are calculated based on Thompson and Eidhammer, 2014 based on the concentrations at lower levels.

Supplementary References

1. Lu, C. H., Liu, Q., Wei, S. W., Johnson, B. T., Dang, C., Stegmann, P. G., Grogan, D., Ge, G., Hu, M., and Lueken, M.: The Aerosol Module in the Community Radiative Transfer Model (v2. 2 and v2. 3): accounting for aerosol transmittance effects on the radiance observation operator, Geosci. Model Dev., 15, 1317-1329, https://doi.org/10.5194/gmd-15-1317-2022, 2022.

2. Schlemmer, L. and Hohenegger, C.: The formation of wider and deeper clouds as a result of cold-pool dynamics, J. Atmos. Sci., 71, 2842-2858, https://doi.org/10.1175/JAS-D-13-0170.1, 2014.

3. Thompson, G. and Eidhammer, T.: A study of aerosol impacts on clouds and precipitation development in a large winter cyclone, J. Atmos. Sci., 71, 3636-3658, https://doi.org/10.1175/JAS-D-13-0305.1, 2014.